Supplementary Informations

for

First pyridyl-terminated trigonal-prismatic cobalt(II) cage-like complex as prospective *N*-donor highly paramagnetic *3D*-shaped ligand (probe)

Svetlana A. Belova,[a] Alexander S. Belov,[a] Margarita G. Bugaenko,[a]

Anastasia A. Danshina,[a] Alexey I. Dmitriev,[c] Mikhail V. Zhidkov,[c]

Denis V. Korchagin,[c] Yan Z. Voloshin*,[a,b]

[a]Nesmeyanov Institute of Organoelement Compounds of the Russian Academy of Sciences, 28–1 Vavilova st., 119334 Moscow, Russia

[b]Kurnakov Institute of General and Inorganic Chemistry of the Russian Academy of Sciences, 31 Leninsky pr., 119991 Moscow, Russia

[c]Federal Research Center of Problems of Chemical Physics and Medicinal Chemistry of the Russian Academy of Sciences, 142432 Chernogolovka, Moscow Region, Russia

Materials and Methods

The reagents used, $CoCl_2 \cdot 6H_2O$, 4-pyridylboronic acid, triethylamine and organic solvents were obtained commercially (SAF). 3-acetylpyrazoloxime (Pz*OxH*) was prepared as described elsewhere [S1].

Analytical data (C, H, N contents) were obtained with a Carlo Erba model 1106 microanalyzer.

MALDI-TOF mass spectra of the obtained monocapped cobalt(II) complex were recorded in the positive and negative ranges with a MALDI-TOF-MS Bruker Autoflex II (Bruker Daltonics) mass spectrometer in a reflecto-mol mode. The ionization was induced by an UV-laser with the wavelength of 337 nm. Its sample was applied to a stainless steel plate and 2,5-dihydroxybenzoic acid was used as the matrix. The accuracy of measurements was 0.1%.

^{1}H NMR spectrum (Fig. S3) was recorded from its solution in CD_2Cl_2 with a Bruker Avance 600 spectrometer. The measurements were done using the residual signals of CD_2Cl_2 (^{1}H 5.32 ppm). In the case of a titration of the complex $[Co(PzOx)_3(B\text{-}4Py)]Cl$ with trifluoroacetic acid, the solution ^{1}H NMR spectra in $CDCl_3$ were recorded with a Varian Inova 400 spectrometer.

Solution UV-Vis spectrum of $[Co(PzOx)_3(B4\text{-}Py)Cl]$ in dichloromethane was recorded in the range 230 – 800 nm with a Varian Cary 60 spectrophotometer. The individual Gaussian components of this spectrum were calculated using the Fityk program [S2].

Synthesis, analytical and spectral characteristics of the complex [Co(PzOx)$_3$(B4-Py)Cl]

$CoCl_2 \cdot 6H_2O$ (0.21 g, 0.90 mmol) and 3-acetylpyrazoloxime (0.40 g, 3.1 mmol) were dissolved in ethanol (7 ml). The solution was heated up to 50°C and 4-pyridylboronic acid (0.14 g, 1.0 mmol) was added to the intensively stirring reaction mixture in two portions. It was refluxed for 10 min, then cooled to r.t. and triethylamine (0.14 ml, 1.0 mmol) was added. Thus obtained mixture was additionally stirred for 10 min and the precipitate formed was filtered off. It was washed with ethanol (15 ml, in three portions), diethyl ether (5 ml) and then extracted with chloroform (10 ml, in two portions). The combined extract was filtered, evaporated to dryness and dried *in vacuo*. Yield: 0.29 g (58%). Anal. Calcd. for $C_{20}H_{22}N_{10}O_3BClCo$ (%): C, 43.23; H, 3.99; N, 25.21. Found (%): C, 43.08; H, 3.81; N, 25.35. MS (MALDI-TOF): *m/z*: 520 [M – $Cl^-]^+$. ^1H NMR (CD_2Cl_2, δ, ppm): –14.01 (br s, 9H, CH_3), –7.04 (br s, 3H, 4-Pz), 34.53 (br s, 2H, *meta*-Py), 74.19 (br s, 2H, *ortho*-Py), 84.53 (br s, 3H, 5-Pz), 270.27 (br s, 3H, NH). Deconvoluted UV-vis (CH_2Cl_2): ν, cm^{-1} (ε × 10^{-3}, mol^{-1} L cm^{-1}): 40355(7.8), 39850(21), 35120(2.7), 31670(3.0), 23740(0.11).

X-ray crystallography experiment

Single crystals of the complex [Co(PzOx)$_3$(B4-Py)Cl]·$CHCl_3$ were grown at room temperature from its saturated solutions in chloroform – heptane 1:3 mixture. Single-crystal XRD data a given the solvatocomplex were collected at 120 K with a Bruker APEXII DUO diffractometer using graphite monochromated Mo-Kα radiation (λ = 0.71073 Å, ω-scans). Its

structure was solved using the Intrinsic Phasing method from the ShelXT [S3] structure solution program in Olex2 [S4] and refined with the XL refinement package [S5] using Least-Squares minimization against F^2 in the anisotropic approximation for non-hydrogen atoms. Hydrogen atoms of the pyrazol NH-groups were found in the difference Fourier synthesis, while the positions of other hydrogen atoms were calculated and all of them were refined in an isotropic approximation. Crystal data and structure refinement parameters for the aforementioned crystal are given in Table S1; CCDC 2416120.

Magnetic measurements

dc experiments

The temperature plots of magnetic moment $M(T)$ and those on the magnetic field flux density {magnetic induction $M(B)$} were measured from the fine-crystalline sample of the cobalt(II) complex $[Co(PzOx)_3(B4\text{-}Py)Cl]$. Initially, it was mixed with an oil Fomblin YR 1800 to avoid the effects of magnetic texturing and then placed into a polyethylene capsule. These measurements were performed using a vibrating sample magnetometer of the multifunctional cryomagnetic measurement system CFMS (Cryogenic, UK) in the temperature range 2 – 300 K at a constant magnetic field of H = 5 kOe. The temperature scan rate was 2 K/min. Thus obtained values of M for the aforementioned sample were corrected to take into account the diamagnetic contributions of the sample holder and of the capsule as well. They were converted into the molar magnetic susceptibility χ_M using Eq. S1: $\chi_M = M/(H\nu)$ (1), where ν is the substance amount and H is the magnetic field strength.

ac experiments

The frequency dependences of the real and imaginary parts of the magnetic susceptibility were measured in a zero constant magnetic field at temperatures of 8 – 20 K in the frequency range of 10 - 10000 Hz. The amplitude of the alternating magnetic field was 4 Oe.

Computational details

Quantum chemical calculations of the electronic structure and spin Hamiltonian parameters for the cage-like complex [Co(PzOx)$_3$(B4-Py)Cl] were performed using a post-Hartree–Fock multi-reference wavefunction approach based on state-averaged complete active space self-consistent field calculations (SA-CASSCF) followed by N-electron valence second-order perturbation theory (NEVPT2) [S9]. Scalar relativistic effects were account for using a standard second-order Douglas–Kroll–Hess (DKH) procedure [S10]. For the aforementioned calculations, a segmented all-electron relativistically contracted version [S11] of Ahlrichs polarized triple-zeta basis set, def2-TZVP [S12], was used for all atoms. To decrease the calculation time, the resolution of the identity approximation with corresponding correlation fitting of the basis set [S13] was applied. SOC effects were included using the quasi-degenerate perturbation theory (QDPT) [S14]. The CASSCF active space was constructed from 5 MOs with predominant contributions of 3d-AOs from the Co center and 7 electrons, corresponding to the cobalt(II) ion CAS(7, 5). Ten quartets and 40 doublet states were included in such calculation. Splitting of the *3d*-orbitals of an encapsulated cobalt(II) ion in the molecule [Co(PzOx)$_3$(B4-Py)Cl] was analyzed within the *ab initio* ligand field theory (AILFT)

[S15]. All quantum chemical calculations were performed with the ORCA program package [S16].

Powder XRD experiment and calculations

PXRD pattern for the fine-crystalline sample of $[Co(PzOx)_3(BC_5H_4NCl]\cdot CHCl_3$ shown in Fig. S8 was measured at room temperature using a Bruker D8 Advance diffractometer equipped with a LynxEye detector and Ge(111) monochromator in a reflection modes. All modeling and indexing were performed using the TOPAS 4.2 software [S17]. Fundamental parameters approach [S18] was used for the profile fitting. The preferred orientation was taken into account with the spherical harmonics approach [S19].

Solution ^{1}H NMR study of protonation of $[Co(PzOx)_3(B4\text{-}Py)Cl]$

The observed changes in the chemical shifts for ^{1}H NMR signals of protons of a given *3D*-shaped molecule (Fig. S4 and Table S3), caused by addition of 5 equivalents of trifluoroacetic acid, were in the range 0.44 – 0.77ppm. The signal of proton of NH^+ group appeared at approximately 40ppm after addition of 1 equivalent of CF_3COOH, thus suggesting a protonation of its apical pyridyl substituent. Such protonation is clearly affected the positions of ^{1}H NMR signals for all other types of protons of this substituent.

Table S1. Crystallographic data and refinement parameters for the crystal $[Co(PzOx)_3(B4\text{-}Py)Cl]\cdot CHCl_3$

Parameter	
Empirical formula	$C_{21}H_{23}BCl_4N_{10}O_3Co$
Formula weight	675.03
T (K)	120
Crystal system	Monoclinic
Space group	$P2_1/c$
Z	4
a (Å)	15.3889(17)
b (Å)	8.0081(9)
c (Å)	22.785(3)
a (°)	90
b (°)	96.665(3)
γ (°)	90
V (Å^3)	2788.9(5)
D_{calc} (g·cm^{-3})	1.608
Linear absorption, μ (cm^{-1})	10.44
F(000)	1372
$2\Theta_{max}$ (°)	56
Reflections measured	20009
Independent reflections	6704
Observed reflections [I>2σ(I)]	5450
Parameters	364
R1	0.0604
wR2	0.1774
GOF	1.060
$\Delta\rho_{max}$/ $\Delta\rho_{min}$ (e Å^{-3})	1.023/–1.035

Table S2. Selected geometrical parameters of the cage-like molecule $[Co(PzOx)_3(B4\text{-}Py)Cl]$

Parameter	
Co – N1 (Å)	2.145(3)
Co – N2 (Å)	2.165(3)
Co – N4 (Å)	2.147(3)
Co – N5 (Å)	2.136(3)
Co – N7 (Å)	2.129(3)
Co – N8 (Å)	2.157(3)
N – O (Å)	1.378(3) –1.384(3) *av.* 1.381
B – O (Å)	1.484(4) –1.492(5) *av.* 1.488
C=N (Å)	1.282(4) – 1.288(5) *av.* 1.284
C – C (Å)	1.457(4) –1.468(4) *av.* 1.462
N=C – C=N (°)	0.5(4) – 8.0(4) *av.* 3.8
NH…Cl (Å)	3.096(3) – 3.159(3)
∠NH – Cl(°)	160.89(19) – 172.9(2)
[a]φ (°)	1.15(16) – 1.41(15) *av*. 1.26
[a]h (Å)	2.570(2)
[a]α (°)	73.4 – 74.2 *av*. 73.8
Co…Cl (Å)	4.6257(11)

[a]φ and h are the distortion angle and the height of TP–TAP coordination polyhedron, respectively; α is the bite (chelate N–Co–N) angle.

Table S3. Symmetry measures of *CoN_6*-coordination polyhedron in the molecule [Co(PzOx)$_3$(B4-Py)Cl] and those for its other *3d*-metal-centered cage-like analogs

Co(II) complex	[Co(PzOx)$_3$ (B4-Py)Cl]	[Co(PzOx)$_3$ (BC$_6$H$_5$)Cl][1a]	[Co(AcPyOx)$_3$ (BC$_6$H$_4$CH$_2$Br)](ClO$_4$) [1c]	[Co(AcPyOx)$_3$ (BFc)](ClO$_4$) [1c]	[Co(AcPyOx)$_3$ (BC$_6$H$_4$CH$_2$SSO$_2$CH$_3$)] (ClO$_4$) [1c]	Co(ImOx)$_3$ (BC$_6$H$_5$)[1d]	Co(ImOx)$_3$ (BC$_6$H$_5$CH$_3$)[1d]	Co(ImOx)$_3$ (BC$_6$H$_5$C$_2$H$_5$)[1d]	[Co(ImOx)$_3$ (BC$_6$H$_5$-*n*-C$_3$H$_7$][1d]
S(HP-6)	35.439	34.069	35.453	36.023	36.073	35.522	35.419	35.374	35.500
S(PPY-6)	16.339	15.647	16.749	17.207	17.176	16.348	16.035	16.092	16.196
S(TAP-6)	16.363	16.271	10.425	9.836	8.878	14.258	14.355	15.454	14.916
S(TRP-6)	0.813	0.827	1.908	2.101	2.700	0.786	0.726	0.653	0.685
S(JPPY-6)	20.301	19.083	20.136	20.136	20.552	20.188	20.301	19.971	20.324
Co(II) complex	[Co(PzOx)$_3$ (BC$_6$H$_5$)Br] · C$_6$H$_6$[1e]	[Co(PzOx)$_3$(BC$_6$H$_5$)Br]·(CH$_2$)$_4$O[1e]	[Co(PzOx)$_3$(BC$_6$H$_5$)Cl] ·CH$_3$COCH$_3$[1e]	[Co(PzOx)$_3$ (BC$_6$H$_5$)Cl] C$_6$H$_6$ [1e]	[Co(PzOx$_3$(BC$_6$H$_5$)Cl] ·CHCl$_3$ [1e]	[Co(FPzOx)$_3$ (BC$_6$H$_5$)Cl] [1e]	[Co(PzOx)$_3$ (BC$_6$H$_5$)Cl] [1e]	{[Co(PzOx)$_3$(BC$_6$H$_5$)I] (69%) + [Co(PzOx)$_3$(BC$_6$H$_5$)Cl] (31%)} ·CHCl$_3$ [1e]	[Co(PzOx)$_3$ (BC$_6$H$_5$)I] [1e]
S(HP-6)	33.494	33.143	35.513	35.157	34.030	34.684	34.402	33.754	35.801
S(PPY-6)	15.167	14.947	16.108	16.407	15.610	16.365	16.053	15.389	16.319
S(TAP-6)	16.651	16.487	15.807	16.330	16.418	16.403	16.099	16.396	15.114
S(TRP-6)	0.932	0.990	0.781	0.815	0.814	0.794	0.822	0.922	0.889
S(JPPY-6)	18.555	18.307	19.884	20.015	19.026	19.990	19.691	18.826	20.414
Complex	[Fe(PzOx)$_3$(BC$_6$H$_5$)Cl] [1a]			[Mn(PzOx)$_3$(BC$_6$H$_5$)Cl] [1a]			[Zn(PzOx)$_3$(BC$_6$H$_5$)Cl] [1a]		
S(HP-6)	35.310			36.092			34.731		
S(PPY-6)	16.440			16.841			15.837		
S(TAP-6)	15.885			16.519			16.533		
S(TRP-6)	1.111			1.563			1.000		
S(JPPY-6)	19.975			20.363			19.324		

[a]S(HP-6), S(PPY-6), S(TAP-6), S(TRP-6) and S(JPPY-6) are the calculated deviations of the geometry of their *MN_6*-coordination polyhedra from an ideal polyhedra: hexagon (HP-6), a pentagonal pyramid (PPY-6), a pseudooctahedron (trigonal antiprism, TAP-6), a trigonal prism (TPR-6) and a Johnson pentagonal pyramid (JPPY-6), respectively.

Table S4. Changes in the values of ^{1}H NMR chemical shifts (ppm) for the signals of protons of the molecule [Co(PzOx)$_3$(B-4Py)Cl] after addition of trifluoroacetic acid.

Type of protons	+ 1 eq of CF_3COOH	+ 5 eq of CF_3COOH
CH_3	+0.33	+0.44
4-Pz	+0.94	+0.74
meta-Py	+0.08	+0.28
ortho-Py	+0.54	+0.77
5-Pz	–0.5	–0.71

Table S5. Energies (cm^{-1}) and Boltzmann populations of five lowest states for the molecule [Co(PzOx)$_3$(B4-Py)Cl] at 300 K according to the performed SA-CASSCF/NEVPT2 calculations

States	Energy	Boltzmann populations
1	0.00	3.80E-01
2	271.76	1.03E-01
3	691.73	1.38E-02
4	1035.95	2.64E-03
5	6776.61	2.92E-15

Table S6. Best fit and calculated (SA-CASSCF/NEVPT2) ZFS parameters, *g*-tensor components and Griffith Hamiltonian parameters for the structurally similar cobalt(II) cage-like complexes in comparison with the geometric parameters[d] of their CoN_6-coordination polyhedra

Parameter	$[Co(PzOx)_3(B4\text{-}Py)Cl]$		$[Co(PzOx)_3(B4\text{-}C_6H_5)Cl]$[a]		$[Co(PzOx)_3(BC_6H_5)Br]\cdot\cdot(CH_2)_4O$ [b]	$Co(PzOx)_3(BC_6H_5)I$ [b]	$[Co(PzOx)_3(BC_6H_5)Cl]\cdot CH_3COCH_3$[b]	$[Co(FPzOx)_3(BC_6H_5)Cl]$[b]	$[Co(AcPyOx)_3(B\text{-}R)]\ (ClO_4)$
	Fit	Calc	Fit	Calc	Fit	Fit	Fit	Fit	Fit
D (cm^{-1})	–104.1(2)	–132.4	–82	–110	-	-	-	-	-
E/D	0.03(1)	0.002	0.003	0.004	-	-	-	-	-
g_z	2.89(3)	3.357	2.9	-	-	-	-	-	-
g_x	2.21(3);	1.848	2.2	-					
g_y	2.21(3)	1.858	2.2	-					
σ	1.3		1.38[b]		1.55	1.58	1.63	1.53	1.19
Δ (cm^{-1})	–567		–387[b]		–521	–627	–259	–129	–1237
h (Å)	2.570		2.574		2.572	2.573	2.583	2.584	2.52 – 2.54
φ (°)	1.2 – 1.4		3.0		1.2	3.8	2.7	1.2	20.0 – 25.5
U_{eff} (K)	145 (205)		214.9		212.6	156.8	219.8	219.0	90

[a] the data from [S6].

[b] the data from [S7].

[c] the data from [S8] (R= $C_6H_4CH_2Br$, ferrocenyl, $C_6H_4CH_2SSO_2CH_3$)

[d] φ and h are the distortion angle and the height of a given TP–TAP coordination polyhedron, respectively.

Table S7. Values of relaxation time (s) at various temperatures (K)

T	τ
8	0.02314
9	0.01661
10	0.0063
11	0.00271
12	0.00188
13	0.00114
14	7.2293E-4
15	4.23567E-4
16	2.51592E-4
17	1.52866E-4
18	9.55414E-5
19	5.57325E-5
20	2.38854E-5

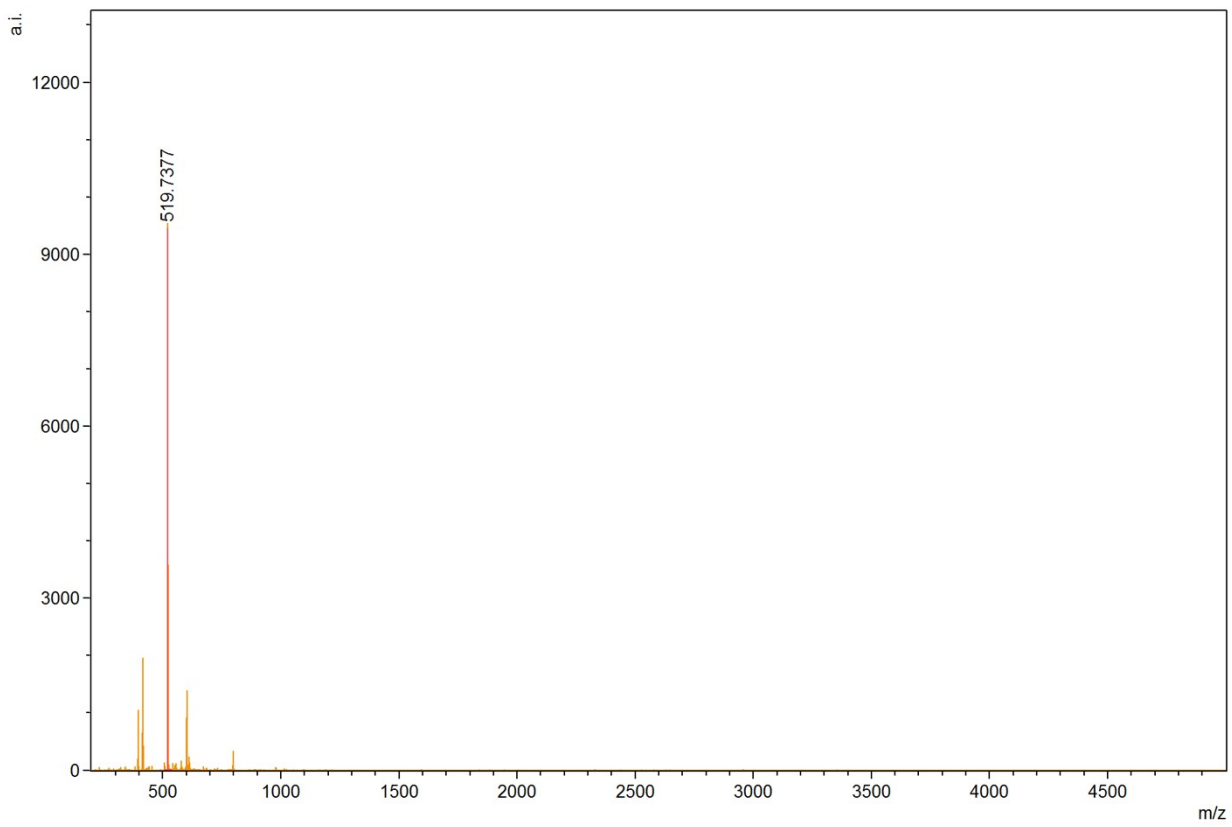

Figure S1. MALDI-TOF mass-spectrum of the complex $[Co(PzOx)_3(B4\text{-}Py)Cl]\cdot$ in its positive range.

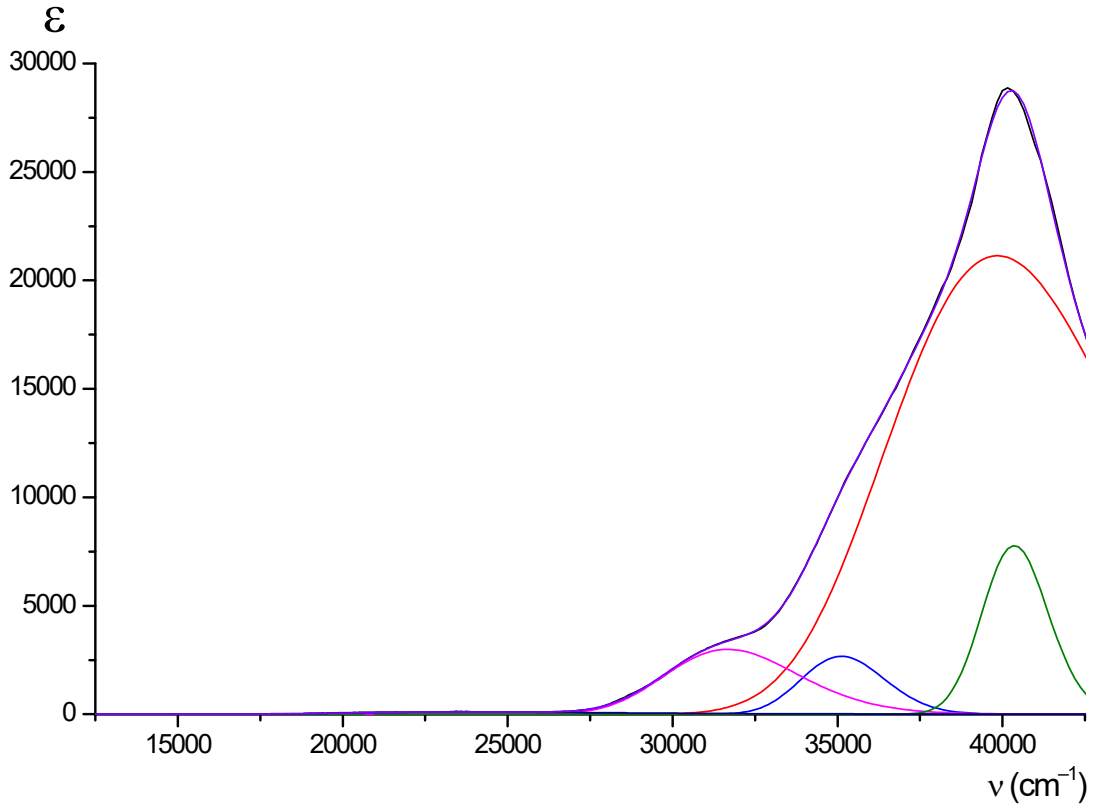

Figure S2. Solution UV-vis spectrum of the complex $[Co(PzOx)_3(B4\text{-}Py)Cl]\cdot$in dichloromethane (shown in black) and its deconvolution into Gaussian components (shown in colour lines).

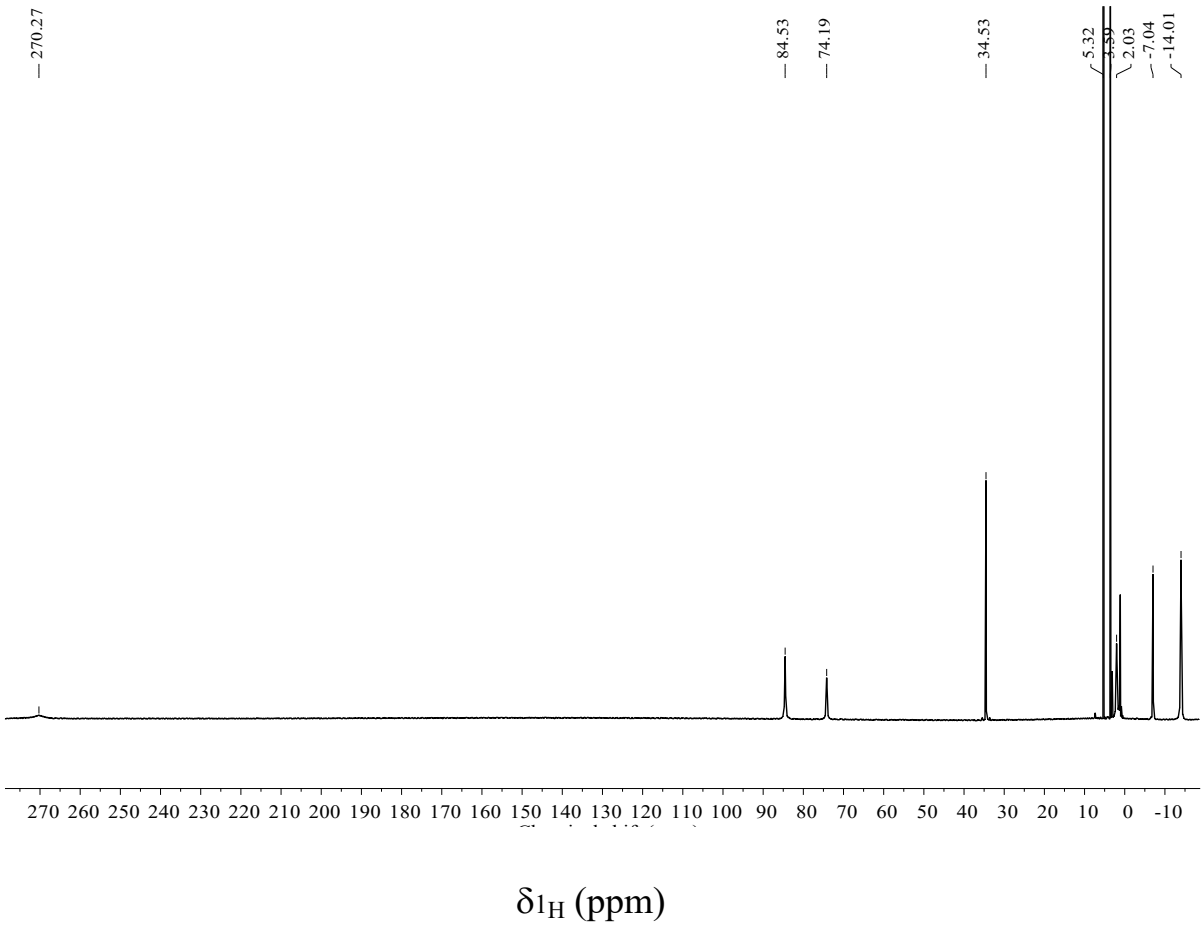

Figure S3. Solution ^{1}H NMR spectrum of the complex $[Co(PzOx)_3(B4\text{-}Py)Cl]\cdot$in CD_2Cl_2.

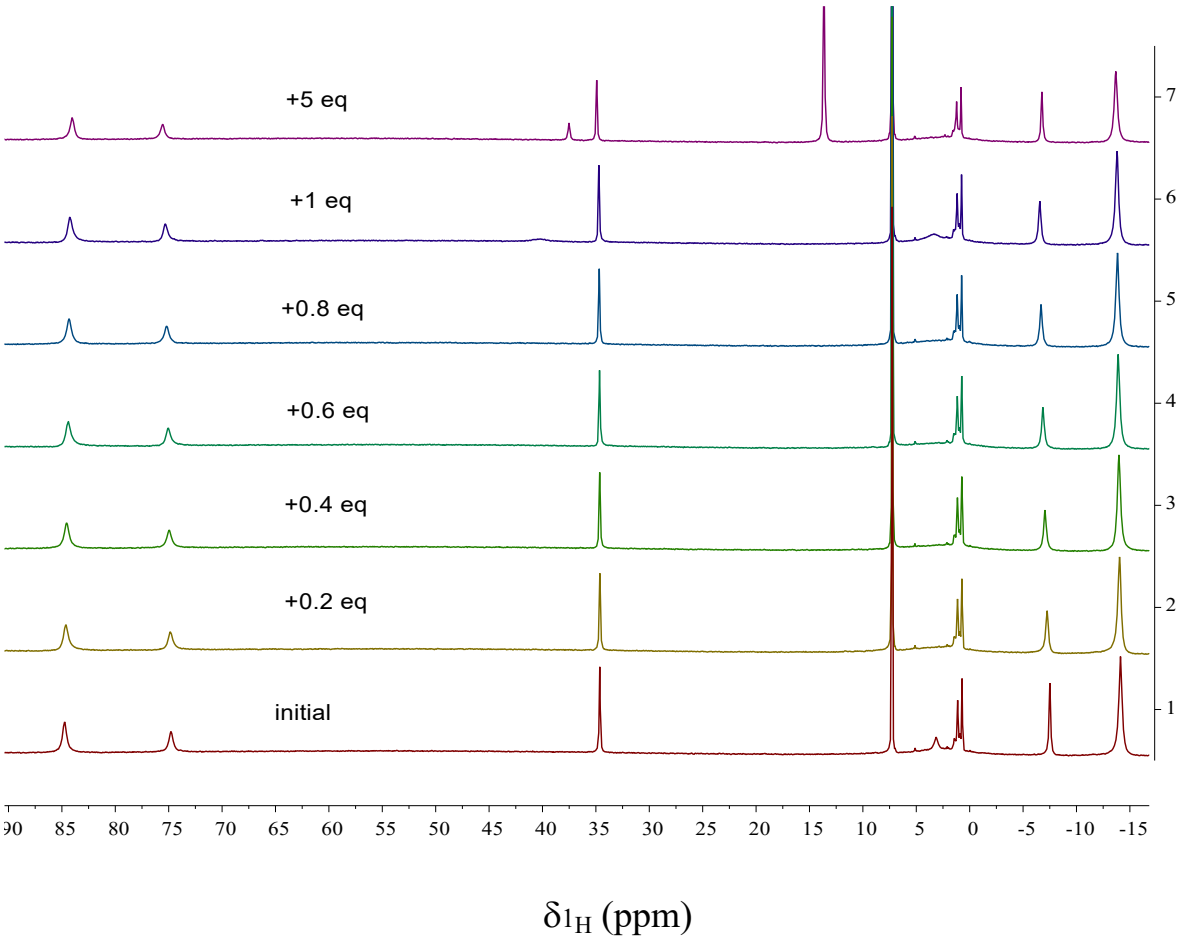

Figure S4. Solution ^{1}H NMR titration of the complex $[Co(PzOx)_3(B\text{-}4Py)Cl]$ with trifluoroacetic acid in $CDCl_3$.

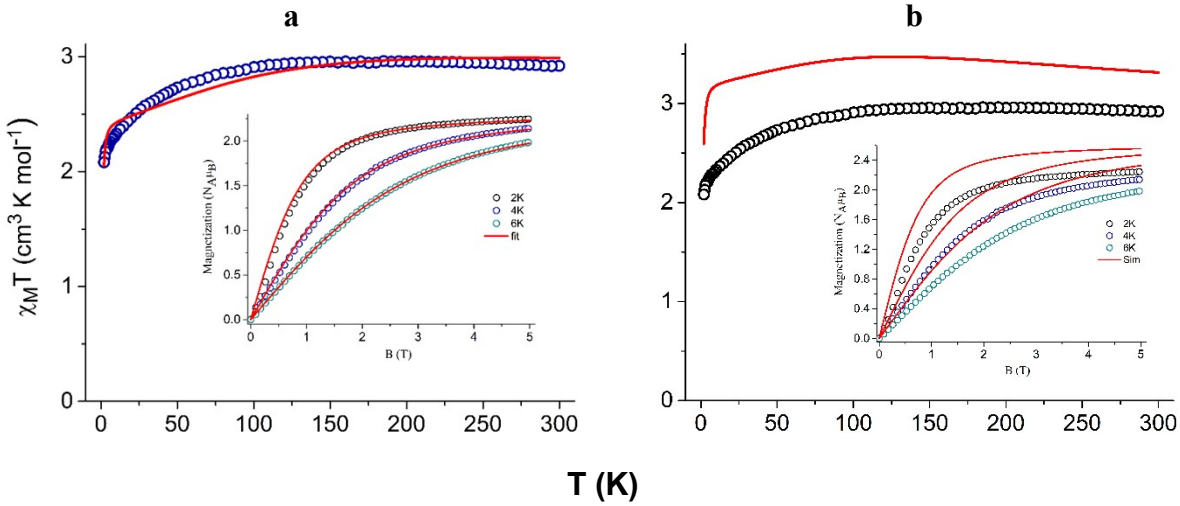

Figure S5. Temperature dependence of $\chi_M T$ for the complex [Co(PzOx)$_3$(B-4Py)Cl] measured at B= 0.5 T (black open circles). Inset: the magnetization vs magnetic field for the complex [Co(PzOx)$_3$(B-4Py)Cl] measured at T =2, 4 and 6 K (open circles).

(a) Theoretical curves (solid red lines) are fitted with the best fit parameters of the spin Hamiltonian: D = –104.1(2) cm^{-1}, E/D= 0.03(1), and $g_x = g_y$ = 2.21(3), g_z = 2.89(3).

(b) Theoretical curves (solid red lines) are simulated with the parameters of the spin Hamiltonian obtained from SA-CASSCF/NEVPT2 quantum chemical calculations: D = –132.4 cm^{-1}, E/D= 0.002, and g_x = 1.848, g_y = 1.858, g_z = 3.357.

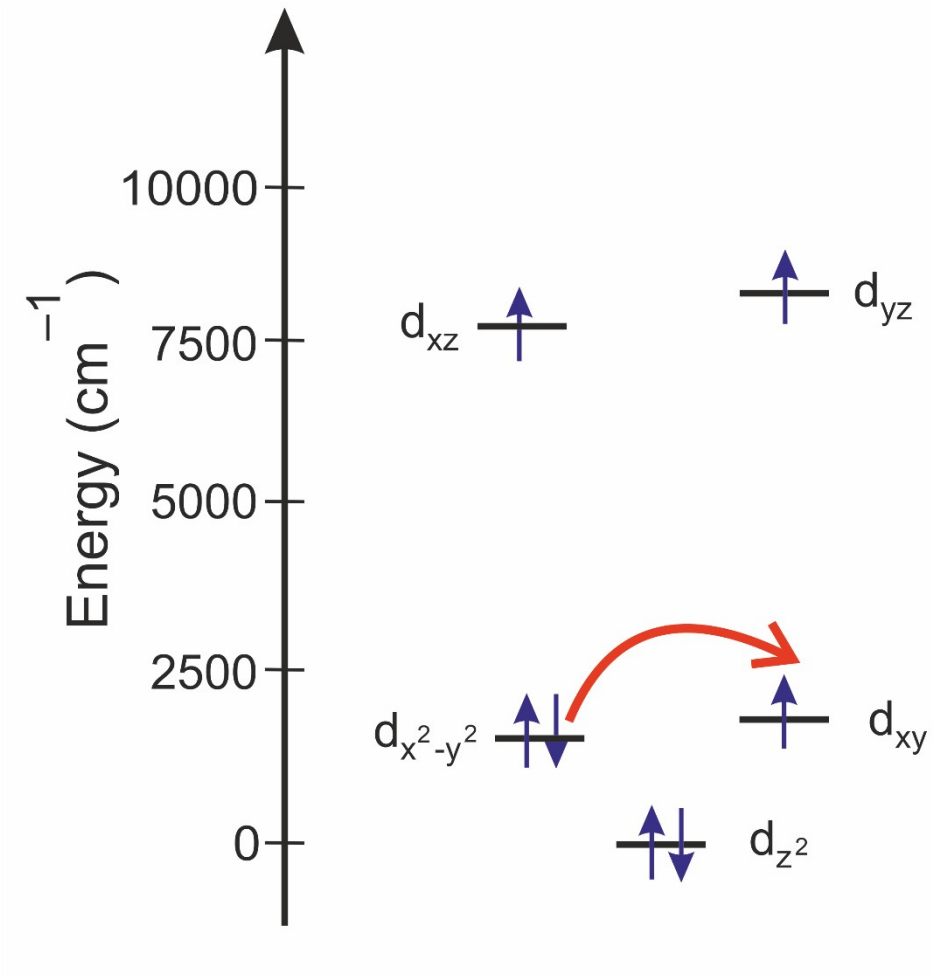

Figure S6. Calculated splitting of *3d*-orbitals of cobalt(II) ion in the cage-like complex [Co(PzOx)$_3$(B4-Py)Cl] (the orbital energies: dz^2=0.0, dx^2–y^2=1468.1, dxy=1780.8, dxz=7589.9, dyz =8152.8 cm^{-1}). Red arrow shows the path to the lowest-lying excited state.

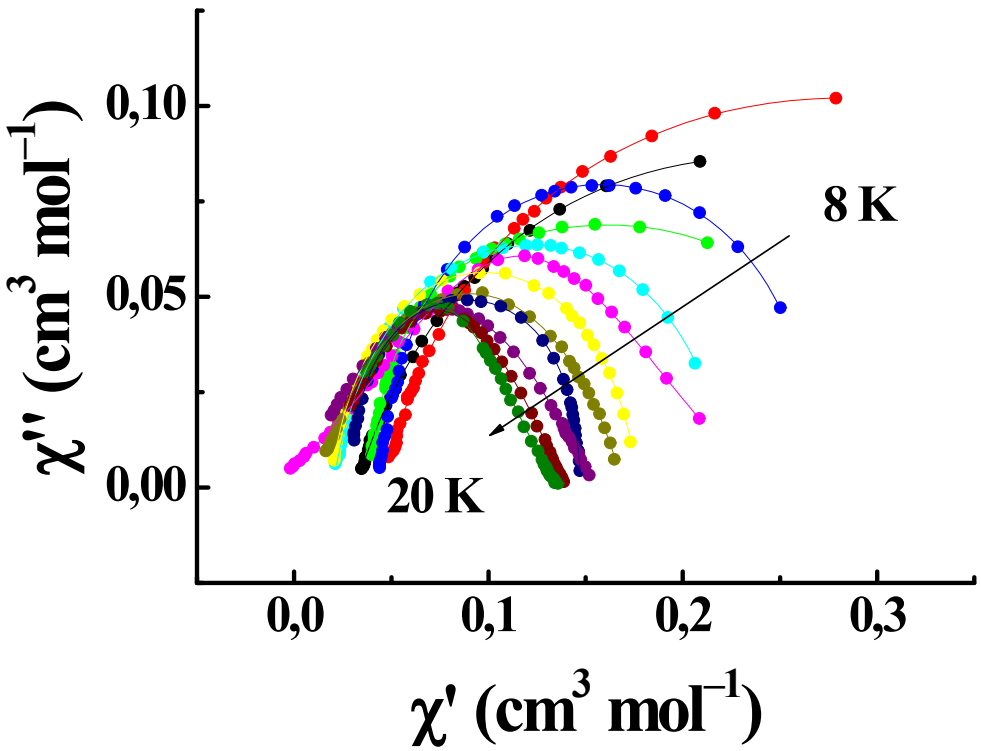

Figure S7. Cole-Cole plots for the complex [Co(PzOx)$_3$(B4-Py)Cl] in zero magnetic field H of 0Oe in the temperature range 8 – 20K. Solid lines demonstrate the approximations by the generalized Debye model.

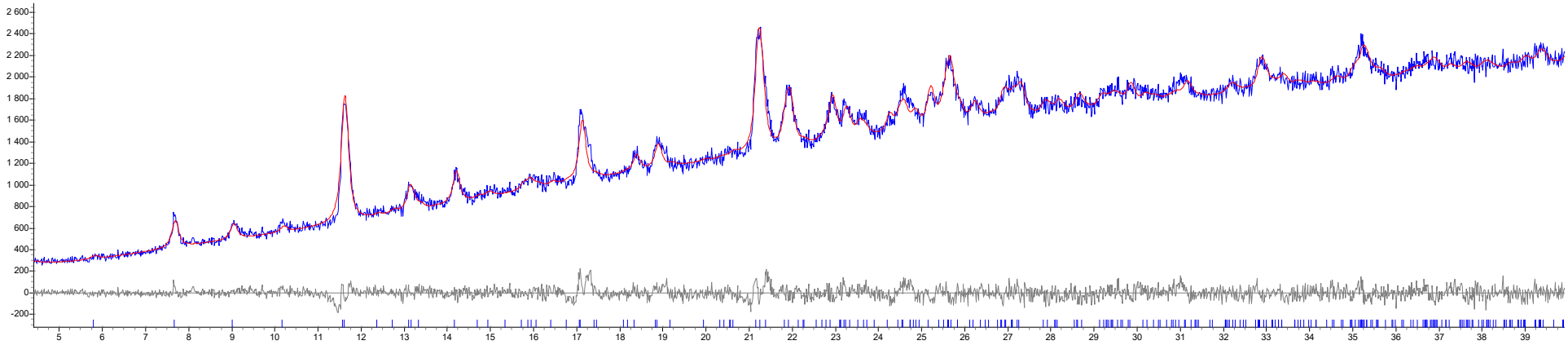

Figure S8. The experimental (shown in blue) and calculated (shown in red) XRD patterns for the complex $[Co(PzOx)_3(BC_5H_4NCl]\cdot CHCl_3$ and the corresponding residual curve (shown in grey). Rietveld refinement confirmed a purity of this sample with Rwp/Rp/Rbragg=3.491/2.636/1.160.

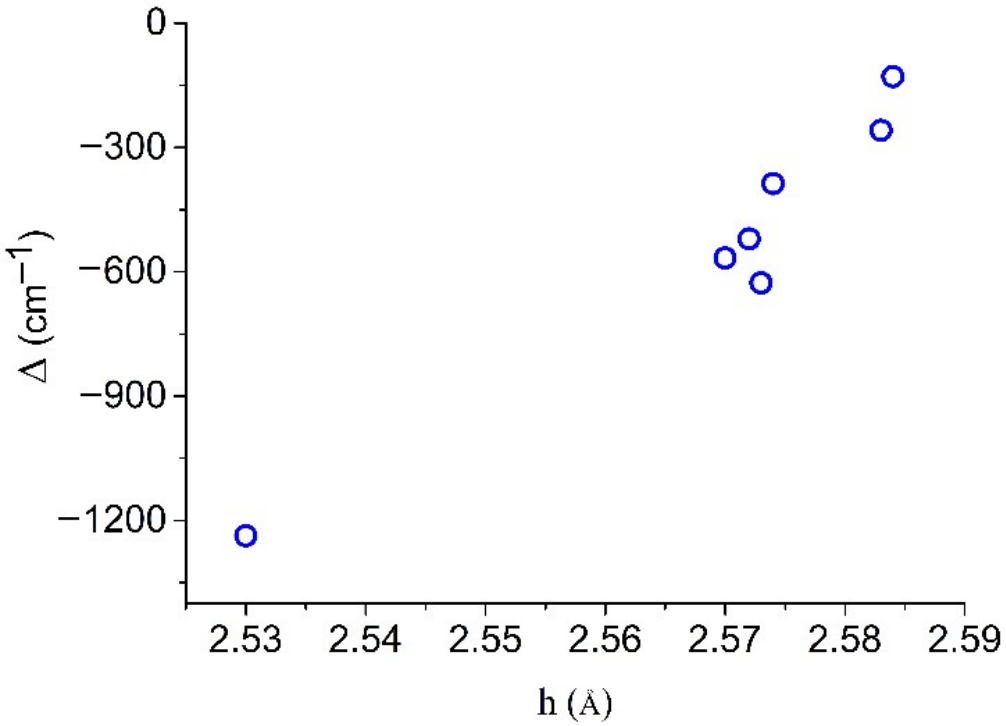

Figure S9. Variation of the axial crystal-field parameter *Δ versus* the height *h* of a TP CoN_6-coordination polyhedron within a series of the structurally similar boron-monocapped cobalt(II) tris-heterocyclooximates (Table S6).

Supplementary Information References

S1. O. A. Varzatskii, S. V. Kats (Menkach), L. V. Penkova, S. V. Volkov, A. V. Dolganov, A. V. Vologzhanina, Y. N. Bubnov, Y. Z. Voloshin, *Eur. J. Inorg. Chem*. (2013) 1987–1992. DOI: 10.1002/ejic.201201545.

S2. M. Wojdyr, *J. Appl. Cryst.* 43 (2010), 1126–1128. DOI: 10.1107/S0021889810030499.

S3. G. M. Sheldrick, *Acta Crystallogr., Sect. A.* 71 (2015) 3−8. DOI: 10.1107/s2053273314026370.

S4. O. V. Dolomanov, L. J. Bourhis, R. J. Gildea, J. A. Howard, H. Puschmann, *J. Appl. Crystallogr*. 42 (2009) 339−341. DOI: 10.1107/S0021889808042726.

S5. G. M. Sheldrick, A Short History of SHELX, *Acta Crystallogr., Sect. A*. 64 (2008) 112–122. DOI: 10.1107/s0108767307043930.

S6. V.V. Novikov, A.A. Pavlov, Y.V. Nelyubina, M.-E. Boulon, O.A. Varzatskii, Y.Z. Voloshin, R.E.P. Winpenny, *J. Am. Chem. Soc*., 137 (2015) 9792−9795. DOI: 10.1021/jacs.5b05739.

S7. S. A. Belova, A. S. Belov, A. A. Danshina, Y. V. Zubavichus, D. Yu. Aleshin, A. A. Pavlov, N. N. Efimov, Y. Z. Voloshin, Dalton Trans. 52 (2024) 1482–1491. 10.1039/d3dt03025c

S8. A. S. Belov, S. A. Belova, N. N. Efimov, V. V. Zlobina, V. V. Novikov, Y. V. Nelyubina, Y. V. Zubavichus, Y. Z. Voloshin, A. A. Pavlov, Dalton Trans. 52 (2023) 2928–2932. DOI: 10.1039/d2dt04073e

S9. (a) C. Angeli, R. Cimiraglia, S. Evangelisti, T. Leininger, J.P. Malrieu, *J. Chem. Phys.*, 114 (2001) 10252-10264; (b) C. Angeli, R. Cimiraglia, J.-P. Malrieu, *Chem. Phys. Lett*., 350 (2001) 297-305; (c) C.

Angeli, R. Cimiraglia, *Theor. Chem. Acc.*, 107 (2002) 313-317; (d) C. Angeli, R. Cimiraglia, J.-P. Malrieu, *J. Chem. Phys.*, 117 (2002) 9138-9153.

S10. B.A. Hess, *Phys. Rev. A*, 33 (1986) 3742-3748.

S11. D.A. Pantazis, X.Y. Chen, C.R. Landis, F. Neese, *J. Chem. Theory Comput.*, 4 (2008) 908.

S12. (a) A. Schafer, C. Huber, R. Ahlrichs, *J. Chem. Phys.*, 100 (1994) 5829-5835; (b) A. Schafer, H. Horn, R. Ahlrichs, *J. Chem. Phys.*, 97 (1992) 2571-2577; (c) F. Weigend, R. Ahlrichs, *Phys. Chem. Chem. Phys.*, 7 (2005) 3297-3305.

S13. F. Neese, *J. Comput. Chem.*, 24 (2003) 1740-1747.

S14. D. Ganyushin, F. Neese, *J. Chem. Phys.*, 125 (2006) 024103.

S15. (a) M. Atanasov, D. Ganyushin, K. Sivalingam and F. Neese, in Molecular Electronic Structures of Transition Metal Complexes II, eds. D. M. P. Mingos, P. Day and J. P. Dahl, Springer Berlin Heidelberg, Berlin, Heidelberg, 2012, pp. 149-220, (b) S. K. Singh, J. Eng, M. Atanasov and F. Neese, Coord. Chem. Rev., 2017, 344, 2-25.

S16. (a) Neese F. *Comput. Molec. Sci.*, 2 (2012) 73-78, doi.org/10.1002/wcms.81; (b). Neese F. *Comput. Molec. Sci.*, 8 (2018) 1-6, doi.org/10.1002/wcms.1327; (c) Neese F., Wennmohs F., Becker U., Riplinger C. *J. Chem. Phys.*, 152 (2020) Art. No. L224108, doi.org/10.1063/5.0004608.

S17. *Bruker TOPAS 5 User Manual*, Bruker AXS GmbH, Karlsruhe, Germany (2014).

S18. R. W. Cheary, A. Coelho, *J. Appl. Crystallogr.*, 25 (1992) 109.

S19. M. Järvinen, *J. Appl. Crystallogr.*, 26 (1993) 525.